ELSEVIER

Biophysical Chemistry 96 (2002) 213–228

Biophysical Chemistry

www.elsevier.com/locate/bpc

Tuning ligand affinity, specificity, and folding stability of an engineered lipocalin variant — a so-called 'anticalin' — using a molecular random approach

Steffen Schlehuber[1], Arne Skerra*

Lehrstuhl für Biologische Chemie, Technische Universität München, Freising-Weihenstephan, Germany

Received 11 June 2001; received in revised form 9 October 2001; accepted 12 October 2001

Abstract

Anticalins are prepared by reshaping the ligand pocket of a natural lipocalin via protein engineering in order to recognize a prescribed ligand. In this manner, the anticalin DigA with specificity for digoxigenin was previously derived from the bilin-binding protein (BBP), a natural lipocalin from *Pieris brassicae*. The four peptide loops that form its ligand-binding site were randomized and a cognate variant was selected from the resulting library. Here, we propose a concept for improving the ligand-binding properties of this anticalin in an in vitro affinity maturation process by step-wise randomization of restricted areas of the loop region. Following selection on digoxigenin-binding activity via phage display and colony screening, several DigA variants were thus obtained. The recombinant proteins were thoroughly characterized in terms of ligand affinity and specificity, secondary structure and thermal stability against unfolding. The variant DigA16/19, which carries several new mutations, exhibits clearly improved affinity for digoxigenin, with $K_D = 12.4$ nM. Hence, it is suitable as a sensitive reagent in biochemical detection experiments, especially when produced as a functional fusion protein with alkaline phosphatase as reporter enzyme. In addition, DigA16/19 possesses enhanced ligand specificity and recognizes part of the linker that was used for fixing the steroid group to a carrier protein. Finally, the digoxigenin-binding anticalins appear to have high physico-chemical stability, with T_m values in the 70 °C range. Our present findings support the notion that anticalins provide a useful class of compact and robust ligand-receptor proteins that can be tailored for practical demands.

Keywords: Anticalin; Bilin-binding protein; Digoxigenin; Ligand binding; Thermal stability

1. Introduction

Anticalins are a novel class of engineered receptor proteins with prescribed ligand specificity derived from the lipocalin fold [1,2]. The anticalin concept arose from the perception that lipocalins, a widespread family of small ligand-transport proteins [3], share certain structural features with antibodies, which serve for the specific recognition of a variety of foreign substances by the immune system. The antigen- or hapten-binding sites of

*Corresponding author. Tel.: +49-8161-714351; fax: +49-8161-714352.

E-mail address: skerra@weihenstephan.de (A. Skerra).

[1] Present address: PIERIS Proteolab AG, Lise-Meitner-Str. 30, 85354 Freising, Germany.

0301-4622/02/$ - see front matter
PII: S0301-4622(02)00026-1

antibodies are composed of six hypervariable loops (also dubbed complementarity-determining regions, CDRs) that are fixed on a conformationally conserved immunoglobulin (Ig) domain framework. Similarly, lipocalins possess a ligand-binding site that is formed by four peptide loops, which are displayed on one side of a structurally rigid β-barrel. Each loop connects one pair of strands in the circularly closed, eight-stranded antiparallel β-sheet which gives rise to this peculiar element of supersecondary structure.

Whereas the β-barrel is highly conserved among the various lipocalins with known three-dimensional structure [2], the set of four loops exhibits remarkable diversity, both in conformation and length, and there is extreme sequence variability within this family. These properties are in agreement with the differing ligand specificities observed for natural lipocalins, depending on the organism or tissue from which they originate. Notably, despite the resemblance with immunoglobulins in terms of their ligand-binding functionality, lipocalins provide several advantages, which raise interest in biotechnology from a practical point of view.

First, lipocalins are much smaller than antibodies or their functional fragments, with a typical molecular size below 20 kDa. Second, they are composed of a single polypeptide chain, so that sources of instability, such as the weak non-covalent association of Ig V_H and V_L domains, are avoided. Third, they are easier to manipulate by genetic engineering, because only one coding region has to be cloned and the simpler set of four variable loops is easier to be mutagenized than six individual CDRs. However, in contrast with antibodies produced by the immune system, lipocalins cannot be built on demand by an organism, following a challenge by foreign substances or invaders. Rather, they are functionally restricted to specialized tasks in their physiological environment, mainly for the transport or storage of poorly soluble or chemically labile compounds within or across tissues.

Consequently, we set out to expand on their apparent potential in ligand-binding capability, which so far seems to be marginally exploited in nature, by reshaping the combining site of a given lipocalin via combinatorial biochemistry and protein design. The bilin-binding protein (BBP) of *Pieris brassicae* served as a model lipocalin in order to randomize a total of 16 amino acid positions in those four loops, which normally form the binding site for biliverdin IX_γ at the open end of the β-barrel [1]. The resulting library of 3.7×10^8 BBP variants was screened for binding activity against several haptenic ligands by means of phage display and colony screening methods. Indeed, engineered lipocalins, then termed anticalins, were isolated with nanomolar affinity values and pronounced specificity for compounds such as fluorescein [1] and digoxigenin [4]. Sequence analysis of the anticalins revealed that all 16 amino acid positions chosen for the randomization process appeared to be highly tolerant towards side chain substitution, thus demonstrating considerable structural plasticity of the lipocalin loop region and ligand-binding site.

Apart from the scientific insight that may be gained from this approach, several practical aspects emerge. In particular, the digoxigenin group constitutes a relevant target both in biochemistry and in medicine. This compound belongs to a group of cardiac glycosides with high therapeutic value [5,6], but also with a rather narrow range of applicable concentrations, so that sensitive and quick methods of quantification are needed. Furthermore, the hydrophilic steroid moiety is increasingly utilized in the field of molecular biology as a non-radioactive label for nucleic acids, proteins and other biomolecules [7–9]. The development of reagents for its sensitive detection will certainly contribute to this technique.

In a preceding study, we succeeded in identifying anticalins from the BBP random library that recognize digoxigenin, together with the closely related digitoxigenin group [4]. The K_D value of the anticalin DigA, which was isolated from the original random library, was 295 ± 37 nM for digoxigenin. In an approach of affinity maturation by selectively randomizing just the first loop of the binding site in this anticalin and subjecting the collection of mutants again to screening for the hapten, the variant DigA16 with significantly enhanced digoxigenin-binding activity was obtained. Both anticalins bound the steroid moiety

irrespective of the chemical substituent attached to C-3 of the ring system, and both exhibited even higher affinity for the related steroid digitoxigenin, which merely differs from digoxigenin by a missing hydroxyl group at C-12.

Here, we report attempts to raise the digoxigenin-binding activity of the cognate anticalin even further by extending the affinity maturation concept to remaining parts of the loop region. In addition, we present data on the ligand specificity and on the biophysical properties of the engineered lipocalins, which will be important in order to assess their potential for practical use.

2. Experimental

2.1. Recombinant DNA methodology

DNA manipulation, bacterial transformation and phagemid production were performed according to standard procedures unless otherwise stated [10–12]. Nucleic acid sequencing was carried out by means of the T7 Sequencing Kit™ (Amersham Pharmacia Biotech, Freiburg, Germany) or on an ABI-Prism™ 310 Genetic Analyzer (Perkin Elmer Applied Biosystems, Weiterstadt, Germany) using the BigDye™ terminator kit. All plasmids employed in this study, either for phagemid display (pBBP24), soluble expression (pBBP21), filter-sandwich colony screening (pBBP22) or biosynthesis of a PhoA fusion protein (pBBP27), were based on the generic $tet^{p/o}$ expression vector pASK75 [13], and their schematic composition has been described [4]. They are mutually compatible in so far as the mutagenized central part of the BBP gene can be conveniently isolated from one plasmid by cutting with *Bst*XI — generating two distinct sticky ends — and directionally inserted into another one.

2.2. Preparation of random libraries

Starting with the gene for the digoxigenin-binding BBP variant DigA16, which had been generated by selection from the original BBP random library, followed by an affinity maturation step [4], two specialized random libraries were constructed by polymerase chain reaction (PCR) in order to mutagenize either loop number 3 or 4 of the binding site. For this purpose, previously described PCR reaction conditions and oligodeoxynucleotides (carrying a mixed base composition in the mutagenized codon positions) were used [1], as well as the primer STS12 (5′-CTT CGA CTG GTC CCA GTA CCA TGG TAA ATG GTG GCA-3′). For the randomization of amino acid residues 88, 90, 93, 95 and 97 in loop number 3, two PCRs (20 cycles) were performed in parallel using pBBP21-DigA16 as template, together with the primer pairs GB2/GB11 or STS12/FS18, respectively. The partially overlapping PCR products (with 183 and 206 base pairs) were isolated by agarose gel electrophoresis, mixed and used as template in the assembly PCR (20 cycles) with the flanking primers STS12 and GB2, resulting in the generation of the full-length gene cassette. The mutagenized DNA fragment (371 bp) was finally isolated, digested with *Bst*XI and ligated with the similarly digested phagemid display vector pBBP24. The ligation mixture containing approximately 17 μg of DNA was used for electroporation of *E. coli* K12 XL1-Blue, yielding ca. 2.2×10^8 transformants. The library for the random mutagenesis of amino acids 114, 116, 125 and 127 in loop number 4 was likewise prepared in a two-step PCR strategy. First, PCR (20 cycles) was carried out using pBBP21-DigA16 as template and STS12/GB4 as primers. The 352-bp fragment was isolated by agarose gel electrophoresis and used as template with the primers STS12/GB2 in a second PCR (20 cycles). The resulting mutagenized 371-bp fragment was subcloned as before, yielding ca. 2.3×10^8 transformants.

2.3. Affinity enrichment by phagemid display

The two mixtures of bacterial transformants harboring pBBP24 with the mutagenized DigA16 genes were separately propagated for each partial library and finally combined prior to the preparation of the phagemids according to a published procedure [4]. DigA16 variants were selected from the mixed phagemid library by panning with a double conjugate of bovine serum albumin (BSA) with digoxigenin and biotin groups, in conjunction with streptavidin paramagnetic beads

(Dynabeads® M-280 Streptavidin, Dynal, Hamburg, Germany) in the following manner. The paramagnetic particles from 100 μl of the commercially available suspension were washed three times with 100 μl of phosphate-buffered saline (PBS: 4 mM KH_2PO_4, 16 mM Na_2HPO_4, 115 mM NaCl) for 1 min and blocked with 100 μl of blocking buffer (PBS containing 0.1% v/v Tween 20 and 2% w/v BSA) for 1 h. A 260-μl aliquot of the freshly prepared phagemid solution in PBS (containing between 4×10^{11} and 1.3×10^{12} phagemids, depending on the panning cycle) was mixed with 40 μl of a 50 nM stock solution of the digoxigenin/biotin–BSA conjugate [4] in PBS and incubated for 1 h. After adding 100 μl of 4× concentrated blocking buffer, the solution was mixed with the drained beads from above and incubated for 10 min. Finally, free binding sites on the streptavidin beads were saturated by adding 10 μl of 4 mM D-desthiobiotin (Sigma, Deisenhofen, Germany) in PBS containing 0.1% v/v Tween 20 (PBS/T). This step also served for avoiding complexation of the *Strep*-tag II [14], which is part of the fusion protein between the BBP variants and the M13 gene III product. Following 5 min of incubation, uncomplexed phagemids were removed by washing of the beads eight times with 1 ml of fresh PBS/T containing 1 mM D-desthiobiotin. Remaining bound phagemids were eluted by treatment with 950 μl of 0.1 M glycine/HCl, pH 2.2 for 15 min. After collection of the beads, the supernatant was recovered and immediately neutralized with 140 μl of 0.5 M Tris base. Subsequent to infection of fresh *E. coli* XL1-Blue cells, the phagemids were either reamplified and used for further panning cycles, or the phasmid DNA was isolated and a filter-sandwich colony screening assay was carried out.

2.4. Filter-sandwich colony screening assay

For the colony screening assay, the mutagenized insert from the pooled phasmid DNA obtained from the phagemid selection was subcloned via *Bst*XI on the vector pBBP22, which encodes a fusion protein between BBP variants and the albumin-binding domain (ABD) from *Streptococcus* protein G [4]. Following transformation of competent *E. coli* TG1/F^- cells with the ligation mixture, the cell suspension was plated out on a hydrophilic filter membrane, placed on an agar plate and subjected to the filter-sandwich colony screening assay as previously described [4]. As a result of this procedure, a second membrane was obtained that carried the functionally immobilized BBP variants as an invisible replica of the colonies grown on the first membrane. These BBP variants were attached via complex formation between the ABD and the human serum albumin (HSA) that had been used for coating of the second membrane. Three membranes of this type were prepared for probing the binding activity of the immobilized DigA16 mutants (corresponding to ca. 500 independent transformants per membrane) by first incubating them with a 0.15 μM solution of the digoxigenin/biotin–BSA conjugate in PBS/T for 1 h. In order to select for variants with slow dissociation rates, the buffer was then replaced by a 2 mM solution of free digoxigenin in PBS. Different stringency was applied by treating the three membranes with the competitor in parallel either for 10 min, for 1 min, or not at all. Finally, all membranes were washed three times with PBS/T and incubated for 1 h with ExtrAvidin®–alkaline phosphatase conjugate (Sigma) diluted 1:10 000 in 10 ml of PBS/T for the detection of digoxigenin/biotin–BSA conjugate that had remained complexed. After final washing steps, a chromogenic reaction was carried out [4]. Colonies corresponding to the most intense signals were identified, recovered from the membrane and propagated, and their plasmid DNA was isolated for further analysis.

2.5. Preparation of soluble anticalins

For the production of the BBP variants, the mutagenized gene cassette was subcloned on pBBP21. *E. coli* JM83 was used for gene expression, which was induced with anhydrotetracycline [13]. Periplasmic secretion was effected via an N-terminal OmpA signal sequence and purification was achieved by means of the C-terminal *Strep*-tag II [14] using streptavidin affinity chromatog-

raphy as previously described [4]. Protein concentrations were determined via A_{280} measurement using extinction coefficients ε_{280} [15] of 54 150 M^{-1} cm^{-1} for the recombinant BBP (corrected for the native protein) and of 53 580 M^{-1} cm^{-1} for the DigA16 mutants. SDS-PAGE was performed using standard slab-gel methodology [16], revealing protein bands by staining with Coomassie brilliant blue R 250 (Roth, Karlsruhe, Germany).

2.6. Fluorescence titration experiments

Fluorescence measurements were carried out with an LS50 B fluorimeter (Perkin Elmer, Norwalk, CT, USA) using a 1×1 cm^2 quartz cuvette thermostatted at 25 °C. Aliquots of the corresponding ligand dissolved in DMF were successively added — up to a final volume of 40 μl, i.e. 2% of the assay solution — to 2 ml of a 1 μM solution of the purified BBP variant in PBS buffer containing 1 mM EDTA (PBS/E). After equilibration for 1 min, the protein fluorescence was excited at a wavelength of 295 nm and the tryptophan emission was measured at 345 nm averaged over 10 s. The data were normalized to an initial fluorescence intensity of 100% and fitted by non-linear least-squares regression with KaleidaGraph software (Synergy Software, Reading, PA, USA) according to the theory of bimolecular complex formation [17].

2.7. CD spectroscopy and thermal denaturation

Circular dichroism spectra of the purified BBP variants were measured with a Jasco J-810 spectropolarimeter (Jasco, Groß-Umstadt, Germany) thermostatted with a computer-controlled water bath. Protein solutions were concentrated at 100–350 μg ml^{-1} in 20 mM Na-phosphate buffer, pH 7.5 and applied in a 1-mm pathlength quartz cuvette sealed with a Teflon lid. Spectra were recorded at 22 °C from 190 to 250 nm (bandwidth 1 nm, scan speed 50 nm min^{-1}) using up to 20-fold accumulation and were corrected for solution blanks. The molar ellipticity was calculated from the raw data according to the following equation:

$$\theta_{MRW}=\frac{\theta_\lambda \cdot M_R}{10 \cdot c \cdot d \cdot N_A}$$

where c denotes the protein concentration [mg ml^{-1}], d is the pathlength [cm], N_A is the number of amino acids (always 184), and M_R is the molecular mass: 21 008 Da for BBP, 20 959 for DigA, 20 808 for DigA16 and 20 800 for DigA16/19.

Thermal unfolding was performed using the same set-up by heating the sample at a constant temperature gradient of 40 K h^{-1} from 20 to between 80 and 95 °C, depending on the protein. Data were collected for each 0.1 K step at wavelengths of 212 or 213 nm, respectively, i.e. where maximal spectral change upon unfolding was observed for each BBP variant. After complete denaturation, the sample was cooled again, using the same constant rate, in order to determine the reversibility of the reaction. The sample buffer showed no change in ellipticity with variation in temperature, so no corrections were made. Data from the thermal denaturation experiments were fitted by non-linear least-squares regression using KaleidaGraph software and an equation for a two-state model of the unfolding transition [18,19]:

$$\theta=\frac{(m_N T+b_N)+(m_U T+b_U)e^{\Delta H_m/R[(1/T_m)-(1/T)]}}{1+e^{\Delta H_m/R[(1/T_m)-(1/T)]}}$$

where m_N, b_N, m_U and b_U denote the parameters for the pre- and post-transitional signal drifts, T is the variable temperature [K], R is the gas constant (8.314 J K^{-1} mol^{-1}), T_m is the melting temperature at the midpoint of transition and ΔH_m is the enthalpy of unfolding [J mol^{-1}] at T_m. Using the parameters from the corresponding curve fit, the unfolded fraction $f(u)$ was plotted as a function of temperature T for illustration:

$$f(u)=\frac{e^{\Delta H_m/R[(1/T_m)-(1/T)]}}{1+e^{\Delta H_m/R[(1/T_m)-(1/T)]}}$$

The Gibbs free energy of unfolding $\Delta G^{o\prime}$ at ambient temperature (25 °C) was extrapolated from T_m (where $\Delta G_U=0$) using simple integration of the van't Hoff equation with a constant ΔH_m:

$$\Delta G^{o\prime}=\Delta H_m\left(1-\frac{298.15\ \mathrm{K}}{T_m}\right)$$

2.8. Preparation and analysis of PhoA fusion proteins

For the production of a fusion protein comprising the bacterial alkaline phosphatase (PhoA) linked to the N-terminus of the BBP variant, the mutagenized gene cassette encoding DigA16/19 was subcloned on the vector pBBP27. The PhoA-DigA16/19 fusion protein was produced in *E. coli* JM83 and purified via the C-terminal *Strep*-tag II, as previously described [4]. Protein concentration was determined using an extinction coefficient $\varepsilon_{280} = 84\,970\ M^{-1}\ cm^{-1}$. ELISA was carried out with the fusion protein following a published procedure [4]. Briefly, the wells of a microtiter plate were coated with digoxigenin groups coupled either to BSA or to ovalbumin (Ova) as carrier protein, using unconjugated proteins for control. After blocking, the PhoA fusion protein was applied in a dilution series and incubated for 1 h. Finally, the wells were thoroughly washed, and enzymatic activity was directly detected by incubation with *p*-nitrophenyl phosphate as chromogenic substrate. The change in absorption at 405 nm was measured in a SpectraMax 250 reader (Molecular Devices, Sunnyvale, CA, USA). The data were fitted by non-linear least-squares regression using KaleidaGraph software, as previously described [20].

3. Results and discussion

3.1. Theoretical considerations and molecular randomization strategy

The BBP library from which the original digoxigenin-binding BBP variant DigA was isolated had been prepared by targeted randomization of a total of 16 amino acid positions. Mutagenesis was achieved by means of a PCR assembly strategy using oligodeoxynucleotides synthesized with mixed bases at the randomized codons. According to the base composition applied (usually 'NNK' or 'NNS'), 32 different codon combinations corresponding to all 20 amino acids were allowed at most of the positions (cf. [1]; at some positions, certain codons/amino acids were avoided, which in principle does not matter for the present discussion). Consequently, the theoretical complexity of this biomolecular library amounted to $32^{16} \approx 1.2 \times 10^{24}$ possible mutants. This number of independent genes or proteins, which would approximately equal 2 moles of substance in total, cannot be physically realized at the present state of the art in molecular biotechnology. In fact, the complexity of 3.7×10^8 independent transformants, which was obtained after preparative ligation of the PCR products and used for preparation of the phagemid display library [1], is not far from the practical upper limit of 10^9–10^{10} mutants that can be currently achieved. Therefore, this number represents just a minute fraction of the amino acid combinations within the ligand pocket of the lipocalin that are theoretically possible. Hence, it is basically beyond expectation to select a variant from this library that may exhibit the 'optimal' binding behavior for the prescribed ligand.

However, once a mutant has been successfully isolated, molecular recognition of the ligand is imprinted to its binding site and its properties may then be further tuned by introducing limited and local structural variations. Along these lines, the variant DigA16 had been prepared on the basis of the DigA biomolecule by once again selectively randomizing loop number 1 in the context of the three other loops, which were kept fixed in their sequences, and subjecting the partially mutant library to a further selection procedure. Since only six residues were mutagenized, the theoretical complexity of the library corresponded to $32^6 \approx 1.1 \times 10^9$ combinations in this case, which could be almost fully sampled in the experiment. With the number of transformants amounting to 1.5×10^9, the library could be expected to cover a significant fraction of the possible combinations following a stochastic estimation [4,21]. Thus, there was reasonable expectation to identify the loop sequence conferring the best ligand affinity in the context of the three other loops, provided that sufficient stringency was employed during the selection steps. As a result, the variant DigA16 exhibited 10-fold higher affinity for digoxigenin than the parental DigA anticalin [4].

Based on these findings, we have now made an attempt to improve the ligand-binding activity of this engineered lipocalin even further by applying another cycle of affinity maturation. However, at this stage it was uncertain which of the remaining loops would be most promising to this end. In the previous experiment, loop number 1 had offered an obvious choice because of its charged amino acid composition in the DigA sequence, which hardly seemed to be ideal for the hydrophilic, but uncharged steroid ligand digoxigenin. Unfortunately, none of the other loops exhibited a similarly salient feature. On the other hand, the ligand pocket of the BBP, providing the scaffold, is rather large and non-symmetric in shape, so that not all of the loops could be expected to be involved in contacts with the ligand to the same extent. Loop numbers 3 and 4 appeared to be spatially closest to the relevant side chains in loop number 1 (Fig. 1), so that their repeated randomization provided the best chance. Therefore, two corresponding partial libraries were prepared, but in order to speed up the process of affinity maturation, no further decision between these two loops was made. Instead, both libraries were combined and it was left to the experiment to select for that mutated loop which would give the larger positive effect on the ligand-binding activity.

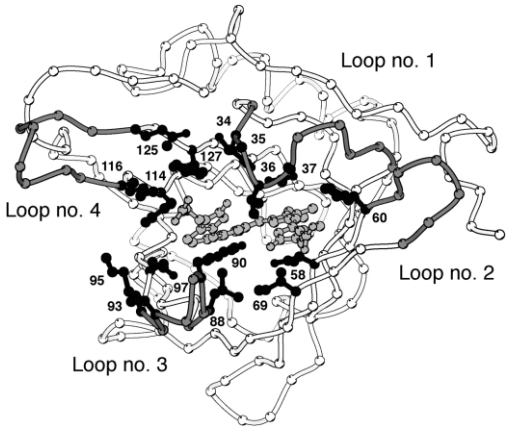

Fig. 1. View into the binding pocket of BBP. The three-dimensional structure determined by X-ray crystallography [22] is shown as a ribbon diagram [25] with the bound natural ligand biliverdin IX_γ depicted in a ball and stick representation (light grey). Apart from the C_α trace (with the four loops colored grey and numbered), the side chains of the 16 initially randomized amino acids are shown (dark grey) and labeled.

3.2. Affinity maturation via targeted random mutagenesis of two loop regions

The preparation of the two libraries took advantage of our previous PCR assembly strategy, albeit in a simpler manner than for the original BBP random library [1]. This time, the DigA16-encoding nucleic acid was utilized as template (Fig. 2). The two resulting PCR fragments, each comprising a gene pool with one mutagenized loop region in the environment of the otherwise unchanged DigA16 sequence, were separately subcloned on a phagemid display vector. After electroporation of *E. coli*, two libraries were obtained, each with approximately 2×10^8 independent transformants. Cultures were inoculated with the bacterial colonies collected in both cases, superinfected with helper phage, and finally combined before performing the phagemid preparation. The phagemids were then subjected to panning against digoxigenin groups [4]. For this purpose, the phagemid solution was incubated with a double conjugate of BSA with digoxigenin and biotin. Compared with the previous selection experiment [4], a 10-fold lower concentration of this double conjugate was applied in order to augment the stringency of selection. Phagemids that had undergone stable complexation with the digoxigenin groups were then recovered via the biotin moiety using streptavidin paramagnetic beads. After several washing steps, these phagemids were finally desorbed by lowering the pH and were used for re-infection of *E. coli*. After propagation, a fresh phagemid solution was prepared and again subjected to the panning procedure.

Altogether four panning cycles were performed until the relative fraction of specifically recovered phagemids remained almost constant (Fig. 3). The phagemids eluted from the fourth cycle were used for infection of *E. coli*, followed by preparation of phasmid DNA from the whole culture. The mutagenized gene insert was excised from the pooled

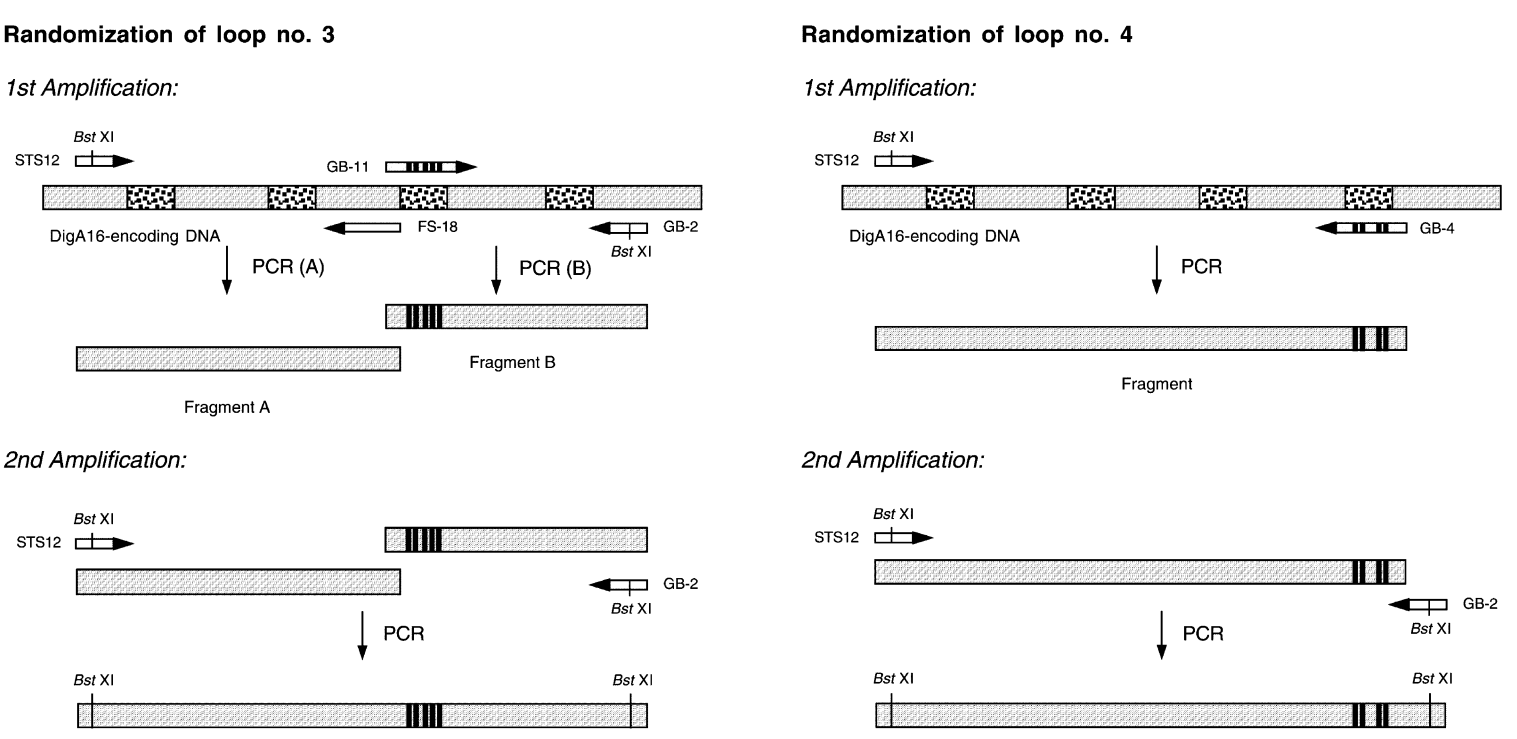

Fig. 2. Strategy for the targeted randomization of the BBP variant DigA16 and resulting DNA sequences of selected variants. (a) Schematic representation of the PCR strategy employed for the construction of two partial libraries concerning either loop number 3 or number 4 (the four loop regions within the gene are dotted). For site-directed random mutagenesis of loop number 3, the structural gene of DigA16 cloned on pBBP21 was used as template in a PCR reaction with the primer GB2 and the degenerate primer GB11, resulting in fragment B. Codons carrying mixed base positions are indicated by black bars. The same template was used in a PCR reaction performed with STS12 and FS18, yielding the partially overlapping fragment A. Both fragments were isolated, combined and employed in a second amplification with the primers STS12 and GB2. Two independent *Bst*XI restriction sites were used for insertion of the randomized gene cassette into pBBP24, a specialized vector for phagemid display. For the randomization of loop number 4, PCR was performed on the same template with STS12 and the degenerate primer GB4. The missing piece contributing one of the *Bst*XI restriction sites was appended in a subsequent amplification with primers STS12 and GB2, followed by cloning as above. (b) DNA sequences and corresponding amino acid translation for the selected variants, in comparison with DigA16. For brevity, sequences are merely shown for amino acid residues 19–138, corresponding to the mutagenized part of the coding region, which is flanked by the *Bst*XI restriction sites ($CCAN_6TGG$, underlined). Amino acid positions that were previously subjected to mutagenesis (see text) are underlined (28, 31, 34-37, 58, 60, 69, 88, 90, 93, 95, 97, 114, 116, 125 and 127). Nucleotides randomized in this study for in vitro affinity maturation are depicted below the DigA16 gene sequence (nomenclature according to NC-IUB [26]). Only the mutated nucleotides with respect to DigA16 and their encoded amino acids are given, whereas identical DNA bases are represented by dots.

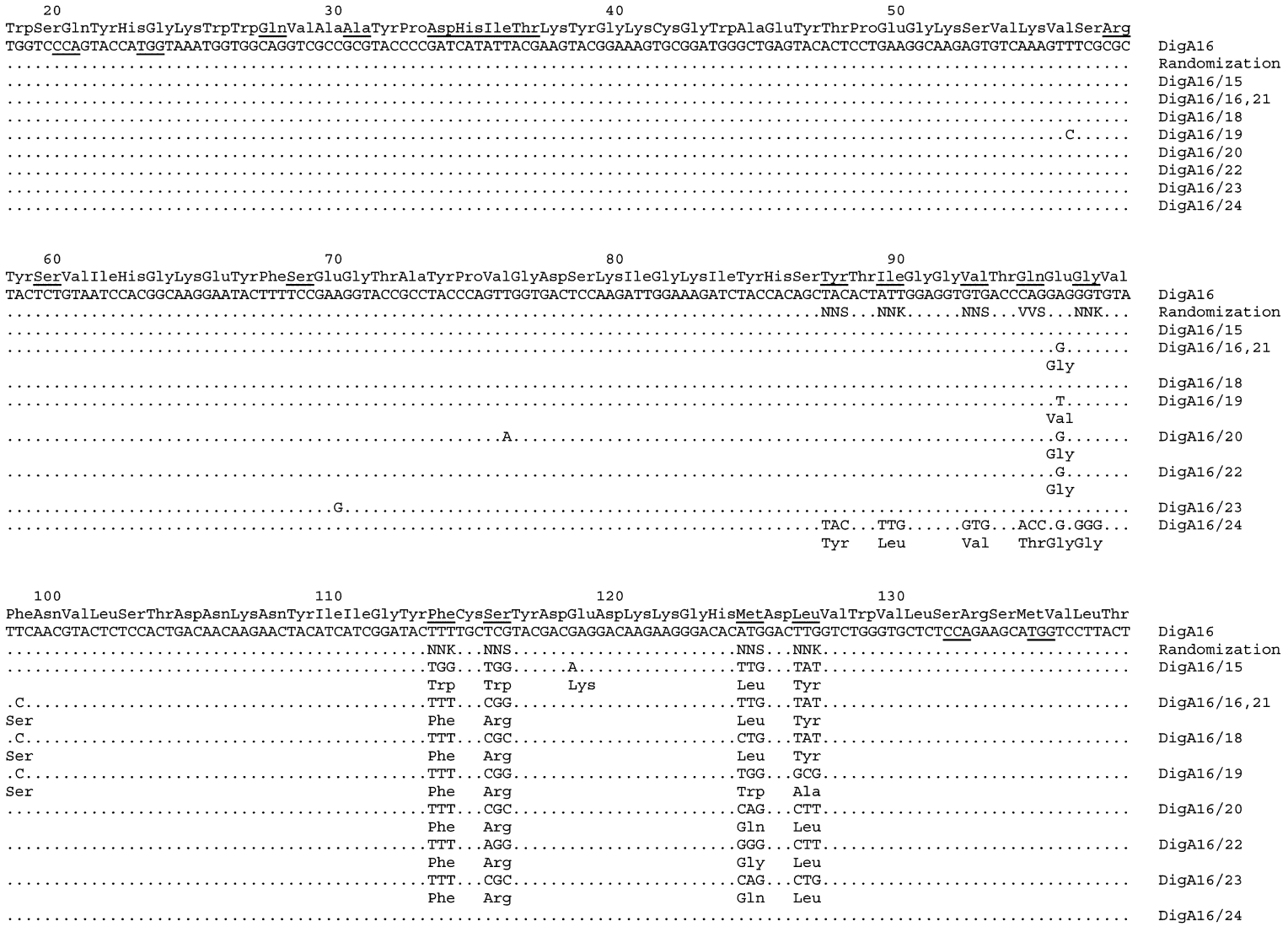

Fig. 2 (Continued).

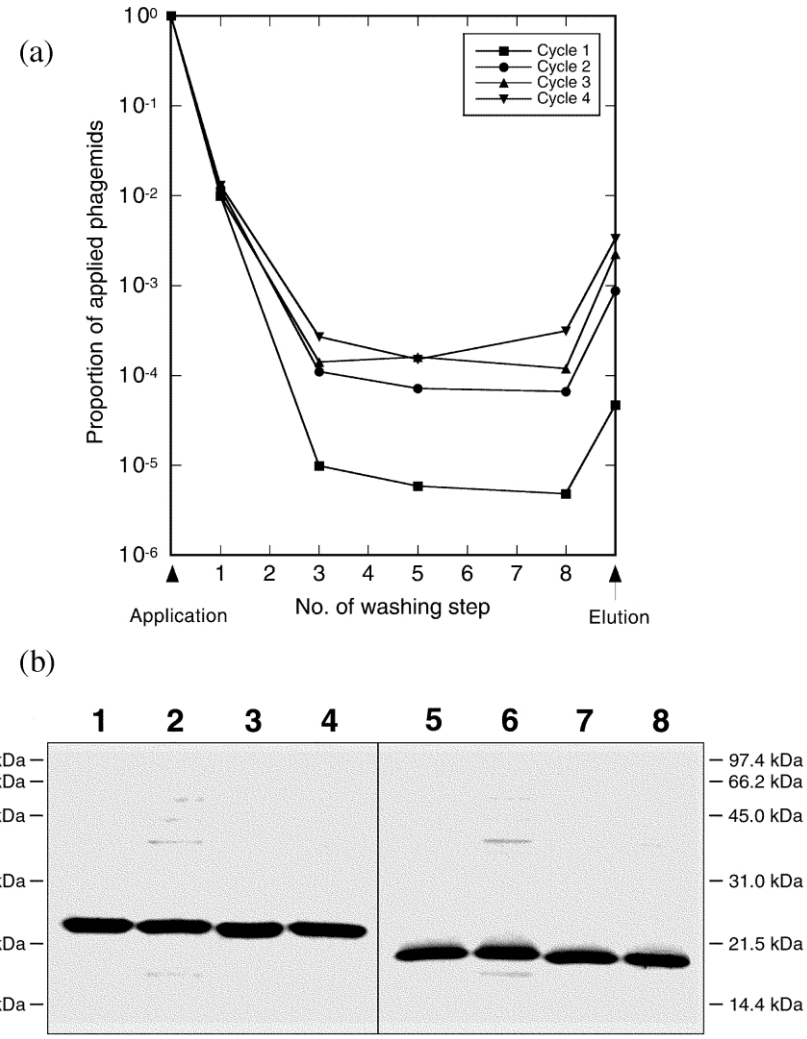

Fig. 3. In vitro affinity maturation of DigA16 by phagemid display and analysis of selected BBP variants by SDS-PAGE. (a) Superposition of the elution profiles from enrichment cycles 1–4 during the selection of DigA16 variants from the combined partial libraries via phagemid display. The phagemid solution was incubated with a digoxigenin/biotin–BSA conjugate and complexed particles were captured by the use of streptavidin-coated paramagnetic beads. After several washing steps, bound phagemids were eluted under acid conditions and subjected to reamplification. The phagemid titers in several of the washing solutions, as well as in the elution sample, were determined and plotted as the relative fraction of the total number of applied phagemids. (b) 15% SDS-PAGE analysis of the BBP variants DigA, DigA16, and DigA16/19. Proteins in lanes 1–4 were treated with mercaptoethanol prior to electrophoresis, whereas proteins in lanes 5–8 were kept unreduced. Recombinant BBP (lanes 1,5), DigA (lanes 2,6), DigA16 (lanes 3,7) and DigA16/19 (lanes 4,8) were prepared by secretion into the periplasm of *E. coli* and purified via the *Strep*-tag II.

DNA and subcloned on a vector that permitted the soluble production of anticalins as fusion proteins with the bacterial albumin-binding domain (ABD). The subpopulation of DigA16 mutants that had been affinity-enriched via phagemid display was then subjected to a filter-sandwich colony screening assay [4]. In this assay, the anticalins, which became secreted from single colonies supported on one filter membrane, were functionally immobilized via the ABD on a second filter membrane

that was previously coated with human serum albumin (HSA). Binding activity was subsequently probed with the digoxigenin/biotin-BSA conjugate, which became specifically complexed in places of colonies where reactive anticalins had been produced. Here, the stringency of detection was further raised by performing a second incubation step with an excess of free digoxigenin for competition, so that the selection was driven for anticalins possessing the slowest dissociation kinetics concerning the bound digoxigenin group (which was still attached to the carrier protein). Digoxigenin/biotin–BSA conjugate that remained complexed to those DigA16 mutants was finally detected by means of an avidin–alkaline phosphatase conjugate.

As a result, nine colonies giving the most intense staining signals were recovered from their filter membrane, were propagated and used for plasmid preparation. Sequence analysis of their mutagenized inserts revealed that a total of eight different variants were present (Fig. 2b). Remarkably, apart from one of the clones (DigA16/24), all variants originated from that fraction of the library where loop number 4 had been randomized. Among those, there was a strong preference for conservation of the Phe residue at position 114 (six of seven clones) and for substitution of Ser^{116} by Arg (six clones). At position 127, the original Leu residue was either retained (three clones) or predominantly replaced by Tyr (three clones). The Met residue at position 125 was preferentially substituted by Leu (three clones) or Gln (two clones). Furthermore, the majority of these clones carried two additional mutations in loop number 3 — at residues which had not been purposely subjected to mutagenesis (cf. Fig. 2) — i.e. at the positions of Glu^{96} (mostly replaced by Gly) and Phe^{99} (always replaced by Ser). These substitutions probably arose from PCR errors during assembly of the genetic library, and they obviously conferred a selective advantage. Even though these seven DigA16 variants exhibited strong similarities in their sequences, the substitution pattern differed in detail, so that all of them were subjected to functional analysis.

3.3. Bacterial production and ligand-binding assays

The genes for the selected DigA16 variants were subcloned on an expression vector for the production of soluble anticalins in *E. coli* [1]. In order to effect efficient disulfide bond formation, the polypeptides were exported into the oxidizing environment of the bacterial periplasm by means of the OmpA signal peptide. Following preparation of the periplasmic cell fraction, the recombinant proteins were isolated in a single step by streptavidin affinity chromatography via the *Strep*-tag II [14] that was fused to their C-terminus. This procedure led to apparently homogeneous protein preparations, whereby the increased electrophoretic mobility in the absence of a thiol-reducing agent indicated proper formation of the pair of disulfide bonds (Fig. 3b). The yield of purified DigA16 mutants varied between 0.1 and 0.8 mg per l culture (harvested at $OD_{550} \approx 1.0$).

The digoxigenin affinity was measured for all variants using the method of fluorescence titration in the same manner as described earlier for the digoxigenin-binding anticalins DigA and DigA16 [4]. Complexation of the hydrophilic steroid was accompanied by significant quenching of the protein's Trp fluorescence (between 27 and 53%, not shown) so that the K_D values could be precisely determined from a curve fit of the fluorescence intensity data with varying ligand concentration (Table 1). The newly selected variant DigA16/19 exhibited the lowest dissociation constant, with $K_D = 12.4 \pm 1.3$ nM. Hence, its affinity was improved almost three-fold compared with the parental DigA16 anticalin. In contrast, the variant DigA16/20 had the highest K_D value, corresponding to an affinity that was almost two-fold lower than that of DigA16. Notably, the two variants with the lowest affinity, DigA16/20 and DigA16/22, carried the accidental $Glu^{96} \rightarrow Gly$ mutation described above, whereas those with the highest affinity, DigA16/19 and DigA16/18, carried the mutation $Phe^{99} \rightarrow Ser$ instead. The single variant where the mutagenesis was directed at loop number 3, DigA16/24, exhibited a mid-range K_D value close to that of the parental DigA16 biomolecule.

Table 1
Digoxigenin affinities of the cognate anticalins as measured by fluorescence titration of the protein ($\lambda_{Ex}=295$ nm; $\lambda_{Em}=345$ nm)

BBP variant	K_D [nM]
BBP	–[a]
DigA	295 ± 37[b]
DigA16	30.2 ± 3.6[b]
DigA16/15	27.2 ± 0.8
DigA16/16	22.5 ± 2.0
DigA16/18	13.9 ± 2.3
DigA16/19	12.4 ± 1.3
DigA16/20	48.2 ± 2.3
DigA16/22	47.0 ± 2.6
DigA16/23	29.2 ± 3.0
DigA16/24	20.3 ± 1.1

[a] No detectable binding activity.
[b] Data from [4].

The apparently successfully optimized variant DigA16/19 was selected for detailed analysis of its ligand specificity. Complexation of several digoxigenin derivatives and related steroids was investigated, again using fluorescence titration of the protein (Table 2). When compared with the corresponding affinity of the original DigA16 anticalin, some interesting features appeared. The affinity of DigA16/19 for digoxin, the natural cardiac glycoside carrying a digitoxose sugar trimer attached to C-3 of the digoxigenin steroid ring system [4], was more than four-fold lower than that for the unsubstituted steroid, demonstrating effective discrimination regarding the substituent at the C-3 position of the ligand. Notably, the same position was used for the attachment of the hydrophilic spacer in the synthesis of the protein conjugates that had been applied during the selection experiments. In contrast, the parental DigA16 variant did not exhibit a detectable difference in the binding of digoxigenin or digoxin. The affinity of DigA16/19 for digitoxigenin, which only differs from digoxigenin by a missing hydroxyl group at C-12, was essentially unchanged compared with DigA16, and with $K_D=2.3\pm0.6$ nM still somewhat better than that for digoxigenin. However, the corresponding glycosylated steroid digitoxin was again bound less tightly by DigA16/19.

Ouabain, on the other hand, a functionally related cardiac steroid glycoside, was not recognized at all, as was previously observed for DigA16. Instead, progesterone was bound with essentially the same reduced affinity, both by DigA16/19 and DigA16. This steroid hormone shows a certain structural resemblance to digoxigenin, in so far as the two methyl residues are preserved at positions C-10 and C-13 and there is also an aliphatic substitutent with the same stereochemistry attached to C-17 in the steroid ring D. Taken together, the second cycle of affinity maturation that was performed in this study resulted in fine-tuning of the affinity and specificity, at least in the case of the anticalin DigA16/19, for the prescribed ligand, and the group attached at the linker position C-3 in the steroid ring A was, for the first time, subject to molecular recognition.

3.4. Secondary structure and thermal stability

Gel filtration experiments with the anticalins indicated that they constituted fully monomeric globular proteins [4]. The secondary structure of the different BBP variants was now investigated by circular dichroism spectroscopy in the far-UV region (Fig. 4). The CD spectra of DigA16/19, DigA16 and DigA essentially revealed the same shape as that of the recombinant BBP. The broad minimum in the region around 210 nm is indicative of a predominant β-sheet structure. In the case of BBP, 48.3% of the residues adopt a β-sheet and 9.7% adopt an α-helical secondary structure, as deduced from crystallographic analysis [22].

Table 2
Dissociation constants for the complexation of digoxigenin derivatives and related steroids by DigA16/19 and its progenitor DigA16 as measured by fluorescence titration ($\lambda_{Ex}=295$ nm; $\lambda_{Em}=345$ nm)

Ligand	K_D [nM]	
	DigA16/19	DigA16
Digoxigenin	12.4 ± 1.3	30.2 ± 3.6[b]
Digoxin	54.9 ± 5.6	31.1 ± 3.2[b]
Digitoxigenin	2.3 ± 0.6	2.0 ± 0.5[b]
Digitoxin	8.4 ± 0.9	3.2 ± 0.5[b]
Progesterone	80.6 ± 3.5	97 ± 15
Ouabain	–[a]	–[a]

[a] No detectable binding activity.
[b] Data from [4].

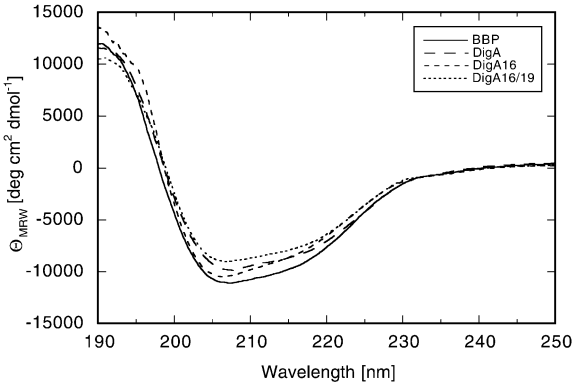

Fig. 4. Superposition of the CD spectra of BBP and its variants DigA, DigA16 and DigA16/19. The spectra were measured in a Jasco J-810 spectropolarimeter at 22 °C in a quartz cuvette with a light path of 1 mm, by accumulating up to 20 single spectra. Proteins were applied at a concentration of 100–350 μg/ml in 20 mM Na-phosphate buffer, pH 7.5. The raw data were used for calculation of the molar ellipticity per amino acid with mean residue weight, Θ_{MRW}, in order to compare the different variants (see Section 2).

Therefore, despite a total of 15 amino acids in DigA, 17 amino acids in DigA16 and 19 amino acids in DigA16/19 being exchanged in comparison with the recombinant BBP, the overall conformation of the polypeptide chain was apparently retained.

CD spectroscopy was also applied in order to investigate the thermal denaturation behavior of the digoxigenin-binding BBP variants. When the protein solution was heated in a physiological buffer to a temperature between 80 and 95 °C, the minimum in the spectrum at approximately 210 nm essentially disappeared (not shown), whereby the maximum in signal difference was detected at 212 or 213 nm, depending on the protein. Consequently, the ellipticity at these wavelengths served as a probe for the unfolding of the protein upon controlled increase in the temperature (Fig. 5). The shape of the denaturation transition was in agreement with a simple two-state model of cooperative unfolding, both for the recombinant BBP and for its variants, DigA, DigA16 and DigA16/19. When lowering the temperature again after thermal denaturation had been accomplished, the transition appeared to be largely reversible, reaching at least 90% of the initial ellipticity at 25 °C and revealing a mid-point temperature within ±2 °C of the T_m value (not shown).

The measured data could be well fitted using the van't Hoff equation [18,19]. From the normalized denaturation curve, it appeared that the recombinant BBP exhibited half-maximal unfolding at $T_m = 61.3$ °C (Table 3). This melting temperature is remarkable for a protein from a mesophilic organism, i.e. the butterfly *Pieris brassicae*. Notably, the T_m values for the digoxigenin-binding variants were even higher, approaching 72.8 °C in the case of DigA. DigA16/19 again exhibited a somewhat lower T_m value of 62.5 °C, i.e. close to the recombinant wild-type protein. However, the individual slopes of the transition, corresponding to the co-operativity of the unfolding event, were slightly different, which is reflected in the varying

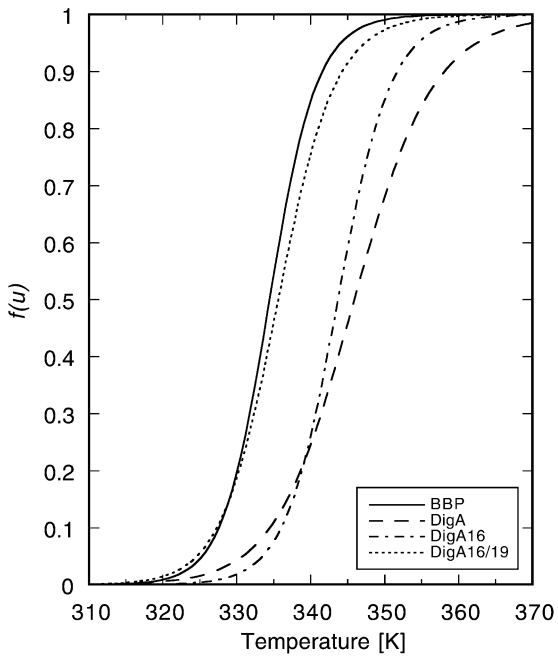

Fig. 5. Thermal denaturation of BBP and its variants DigA, DigA16 and DigA16/19 as determined by CD measurements in the far-UV region. Purified proteins (for conditions cf. Fig. 4) were heated at a constant rate, and the ellipticity was followed at an appropriate wavelength of approximately 212 nm (cf. Table 3) in order to determine the fraction of unfolded protein, $f(u)$. T_m values and thermodynamic parameters ΔH_m and $\Delta G^{o\prime}$ were derived by curve fitting (see Section 2) and are listed in Table 3.

Table 3
Thermodynamic parameters from reversible thermal unfolding experiments as measured by CD

Protein	T_m [°C]	ΔH_m [kJ mol^{-1}]	$\Delta G^{o\prime}$ [kJ mol^{-1}]	λ [nm]
BBP	61.31±0.03	291.9±4.8	31.7±0.5	212
DigA	72.78±0.09	181.2±13.4	25.0±1.9	213
DigA16	70.56±0.06	273.8±17.3	36.3±2.3	212
DigA16/19	62.47±0.06	240.0±8.4	26.8±0.9	212

ΔH_m values (cf. Table 3). Consequently, simple extrapolation of the folded/unfolded equilibrium to ambient temperature resulted in values between 25 and 31 kJ mol^{-1} for the Gibbs free energy of unfolding, $\Delta G^{o\prime}$. In a preliminary study on the chemically induced unfolding of the BBP variants, a similar tendency was observed regarding their relative conformational stability. In this case, DigA16 exhibited a reversible unfolding transition at a midpoint concentration of 1.8 M Gdn·HCl when denaturation was followed via the protein fluorescence (Schlehuber and Skerra, unpublished).

3.5. Construction of a PhoA fusion protein for the detection of digoxigenin groups in an ELISA

A sensitive reagent for the detection of digoxigenin-labeled biomolecules is of considerable practical value. To this end, we constructed a fusion protein of the DigA16/19 anticalin with bacterial alkaline phosphatase (PhoA) as a reporter enzyme. Alkaline phosphatase from *E. coli*, which is a large homodimeric protein, was fused to the N-terminus of the anticalin polypeptide chain, which is well accessible at the outside of the β-barrel structure. The fusion protein was readily produced via secretion into the bacterial periplasm, employing the enzyme's own signal sequence. Purification was achieved by means of the *Strep*-tag II attached to the C-terminus of the anticalin, similarly as described above. The digoxigenin-binding activity of the DigA16/19 fusion protein was then investigated in an ELISA (Fig. 6) and compared with the analogous PhoA fusion of the predecessor DigA16 [4].

As a result, digoxigenin groups displayed either by BSA or by ovalbumin (Ova) as carrier proteins were detected with high signal strength after complex formation with the fusion protein and addition of a standard chromogenic reagent. The signals followed a steep saturation curve, irrespective of whether BSA or ovalbumin was used, and there was virtually no background signal when the underivatized carrier protein served as a control. Notably, the sensitivity of the DigA16/19 fusion protein appeared to be significantly improved in comparison with the parental DigA16 version. In summary, the repeated affinity maturation of the digoxigenin-binding anticalin DigA, which was initially isolated from a BBP random library, has thus yielded a small and robust receptor protein that should be practically useful in biochemical detection experiments.

3.6. Conclusions

Even though the biochemical function of BBP was dramatically changed in the course of the repeated randomization and selection experiments, and more than 10% of its amino acid residues were exchanged, the secondary structure of its

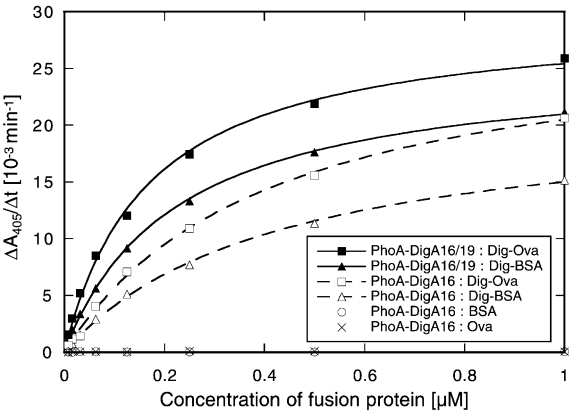

Fig. 6. Detection of digoxigenin groups using the PhoA-DigA16/19 and PhoA-DigA16 fusion proteins. The wells of a microtiter plate were derivatized with a digoxigenin–BSA and –ovalbumin (Ova) conjugate, respectively, or unconjugated carrier protein as a control. Each purified fusion protein was applied in a dilution series and — after adsorption and washing — directly detected via chromogenic reaction. The enzyme activity measured ($\Delta A_{405}/\Delta t$) was plotted against the applied concentration of the fusion protein and subjected to curve fitting.

polypeptide chain remained largely unaltered, as revealed by the CD spectroscopy studies. On the contrary, its conformational stability appeared to be increased, albeit no corresponding selective pressure had been applied in our experiments. Obviously, the high thermal stability constitutes an intrinsic property of the rigid β-barrel architecture. However, the significant rise in the melting temperature for DigA compared with BBP was probably a serendipitous event, given that the T_m was gradually lowered again in the course of the following affinity maturation cycles. Nevertheless, our findings indicate that the stability of an anticalin may in fact be engineered, similarly as with recombinant antibody fragments [23], provided that appropriate selection conditions are used.

Taken together with the preceding study [4], we could demonstrate that the process of in vitro affinity maturation can be successfully applied in order to fine-tune the binding activity and ligand specificity of an anticalin. To this end, an effective imprint of the molecular recognition property for the prescribed ligand onto the binding pocket of the lipocalin is a prerequisite. According to the probability estimates presented above, the four loops of the initially selected protein may subsequently be subjected to randomization/selection procedures one after the other in order to optimize the binding behavior. A similar sequential strategy has been proposed in the context of antibody engineering regarding the six CDRs of an antigen-binding site [24].

Generally, the initial spatial orientation of the ligand within the pocket of the anticalin that was selected from the naive random library is likely to be the limiting factor for the affinity that may finally be achieved. During the selection of digoxigenin-binding anticalins from the BBP random library, just one variant with high ligand affinity, DigA, was identified [4]. If there had been further variants available, most desirably with alternative modes of binding, the affinity maturation could have led to different, and possibly even better results. Therefore, it is crucial to create an initial random library with maximal functional diversity to fully exploit the structural space and to finally generate biomolecules with well-optimized ligand-binding properties.

Depending on the ligand orientation and on the success of the initial selection process, the structural influence of the individual loops on the binding energy should differ, especially in the case of a small haptenic ligand, which may not entirely occupy the extended binding pocket. In the case of the digoxigenin-binding anticalin DigA, loop number 1 apparently exerted the strongest effect during affinity maturation, whereas loop number 4 provided a lower contribution, and loop number 3 probably had an even lesser effect. A similar trend appeared in the decreasing convergence of the corresponding selected sequences. In summary, pronounced preferences were previously observed for the randomized positions in loop number 1, and here for positions in the more buried part of loop number 4, as well as for residue 99 in loop number 3. These findings indicate that the slim steroid moiety is likely to be complexed within the left part of the binding pocket (cf. Fig. 1). Based on this knowledge, additional amino acid residues, apart from those initially chosen for the preparation of the BBP random library, might be considered for variation in future engineering experiments with this anticalin.

Finally, it should be noted that the selection was not performed with the free ligand, but with its macromolecular conjugate. The K_D values determined for the selected DigA16 mutants with the free digoxigenin compound may therefore be somewhat misleading regarding the actual success of the affinity maturation process. Interestingly, the specificity of the present variants selected was clearly changed compared with the parental anticalin DigA, which also points towards increased influence of the spacer group attached to digoxigenin on the molecular recognition.

In conclusion, the method of randomizing individual loops in the context of an otherwise unaltered binding site and selecting improved variants from the resulting mixture should provide a quick, general route to the efficient affinity maturation of anticalins. Given their high folding stability and facile manipulation, the novel class of anticalins provides an obvious benefit in the generation of cognate binding proteins for prescribed ligands, with applications in biotechnology and medicine.

References

[1] G. Beste, F.S. Schmidt, T. Stibora, A. Skerra, Small antibody-like proteins with prescribed ligand specificities derived from the lipocalin fold, Proc. Natl. Acad. Sci. USA 96 (1999) 1898–1903.

[2] A. Skerra, Lipocalins as a scaffold, Biochim. Biophys. Acta 1482 (2000) 337–350.

[3] D.R. Flower, The lipocalin protein family: structure and function, Biochem. J. 318 (1996) 1–14.

[4] S. Schlehuber, G. Beste, A. Skerra, A novel type of receptor protein, based on the lipocalin scaffold, with specificity for digoxigenin, J. Mol. Biol. 297 (2000) 1105–1120.

[5] T.W. Smith, Pharmacokinetics, bioavailability and serum levels of cardiac glycosides, J. Am. Coll. Cardiol. 5 (1985) 43A–50A.

[6] T.W. Smith, Digitalis. Mechanisms of action and clinical use, N. Engl. J. Med. 318 (1988) 358–365.

[7] H.J. Höltke, W. Ankenbauer, K. Mühlegger, et al., The digoxigenin (DIG) system for non-radioactive labelling and detection of nucleic acids — an overview, Cell. Mol. Biol. 41 (1995) 883–905.

[8] T. McCreery, Digoxigenin labelling, Mol. Biotechnol. 7 (1997) 121–124.

[9] J. Chevalier, J. Yi, O. Michel, X.M. Tang, Biotin and digoxigenin as labels for light and electron microscopy in situ hybridization probes: where do we stand?, J. Histochem. Cytochem. 45 (1997) 481–491.

[10] J. Sambrook, E.F. Fritsch, T. Maniatis, Molecular Cloning: A Laboratory Manual, Cold Spring Harbor Laboratory Press, Cold Spring Harbor, New York, 1989.

[11] J.H. Miller, A Short Course in Bacterial Genetics, Cold Spring Harbor Laboratory Press, Cold Spring Harbor, New York, 1992.

[12] B.K. Kay, J. Winter, J. McCafferty, Phage Display of Peptides and Proteins — A Laboratory Manual, Academic Press, San Diego, 1996.

[13] A. Skerra, Use of the tetracycline promoter for the tightly regulated production of a murine antibody fragment in *Escherichia coli*, Gene 151 (1994) 131–135.

[14] A. Skerra, T.G.M. Schmidt, Use of the *Strep*-tag and streptavidin for recombinant protein purification and detection, Methods Enzymol. 326 (2000) 271–304.

[15] S.C. Gill, P.H. von Hippel, Calculation of protein extinction coefficients from amino acid sequence data, Anal. Biochem. 182 (1989) 319–326.

[16] S.P. Fling, D.S. Gregerson, Peptide and protein molecular weight determination by electrophoresis using a high-molarity Tris-buffer system without urea, Anal. Biochem. 155 (1986) 83–88.

[17] M. Vogt, A. Skerra, Bacterially produced apolipoprotein D binds progesterone and arachidonic acid, but not bilirubin or *E*-3M2H, J. Mol. Recognit. 14 (2001) 79–86.

[18] M.H. Nasser Brumano, E. Rogana, H.E. Swaisgood, Thermodynamics of unfolding of β-trypsin at pH 2.8, Arch. Biochem. Biophys. 382 (2000) 57–62.

[19] D.S. Cohen, G.J. Pielak, Stability of yeast iso-1-ferricytochrome *c* as a function of pH and temperature, Protein Sci. 3 (1994) 1253–1260.

[20] S. Voss, A. Skerra, Mutagenesis of a flexible loop in streptavidin leads to higher affinity for the *Strep*-tag II peptide and improved performance in recombinant protein purification, Protein Eng. 10 (1997) 975–982.

[21] G. Schreiber, Ein kombinatorisches Problem aus der Genetik, BioEngineering 2 (1988) 32–35.

[22] R. Huber, M. Schneider, I. Mayr, et al., Molecular structure of the bilin-binding protein (BBP) from *Pieris brassicae* after refinement at 2.0 Å resolution, J. Mol. Biol. 198 (1987) 499–513.

[23] S. Jung, A. Honegger, A. Plückthun, Selection for improved protein stability by phage display, J. Mol. Biol. 294 (1999) 163–180.

[24] C.F. Barbas, D.R. Burton, Selection and evolution of high-affinity human anti-viral antibodies, Trends Biotechnol. 14 (1996) 230–234.

[25] P.J. Kraulis, MOLSCRIPT: a program to produce both detailed and schematic plots of protein structures, J. Appl. Crystallogr. 24 (1991) 946–950.

[26] NC-IUB, Nomenclature for incompletely specified bases in nucleic acid sequences, Eur. J. Biochem. 160 (1985) 1–5.